An appraisal of dwell sensitive fatigue in Ti-6Al-4V and the governing role of inhomogeneous micro-texture

J. Li[1], H.M. Davies[1], K. Fox[2], M. Mulyadi[2], M.G. Glavicic[3] and M.R. Bache[1]

[1.] Institute of Structural Materials, Faculty of Science and Engineering, Swansea University, Swansea, SA1 8EN, UK.

[2.] Rolls-Royce plc, P.O. Box 31, Derby, DE24 8BJ, UK.

[3.] Rolls-Royce Corporation, 450 South Meridian Street, Indianapolis, IN 46225, USA.

Keywords

Ti-6Al-4V; fatigue; dwell sensitivity; microstructurally textured regions; quasi-cleavage facets.

Abstract

The fact that the α/β titanium alloy Ti-6Al-4V is sensitive to cold dwell loading regimes has recently been endorsed by a combination of evidence gathered from fatigue studies performed on laboratory scale specimens and the findings of a failure investigation into an in-service fan disc failure. This work confirms that Ti-6Al-4V can demonstrate dwell characteristics under fatigue loading, subject to the microstructure and micro-texture developed during thermo-mechanical processing. Additional fatigue data are presented to support this conclusion, together with detailed metallographic and crystallographic characterisation to identify the factors controlling inhomogeneous strength, stress distribution and the crack initiation process on the micro to macro scale.

Nomenclature

α	hexagonal structured alpha phase
β	body centred cubic beta phase
CNC	computer encoded control
EBSD	electron back scattered diffraction
IPFZ	inverse pole figure for the plane normal to the Z axis
LCF	low cycle fatigue
HCF	high cycle fatigue
MTR	microstructurally textured region
SEM	scanning electron microscopy

Introduction

The phenomenon of room temperature, dwell sensitive fatigue in titanium alloys was first considered in the early 1970s, a consequence of investigations into well publicised in-service fan disc failures suffered by early variants of the RB-211 engine powering Lockheed Tristar aircraft [1]. As a direct outcome of those investigations a seminal publication by Evans and Gostelow [2], based at the Royal Aircraft Establishment at Farnborough UK, characterised the effects of "dwell fatigue" in the near-α titanium alloy Ti-685, the specific service alloy of concern at that time, utilising laboratory specimens extracted from disc forgings. They quantified a reduction in fatigue lives when the material was

subjected to loading waveforms incorporating a hold at peak applied stress, compared to standard "cyclic" waveforms. The ability of titanium alloys in general to accumulate strain under static loading at room temperature had been recognised since the mid twentieth century [3]. Consequently, the "cold dwell" effect was attributed to the superposition of time dependent creep strain accumulating during the dwell period in addition to conventional fatigue damage.

Detailed inspections of model spin rig disc failures and fractographic studies of conventional laboratory test specimens indicated that dwell fractures often initiated at sub-surface locations from quasi-cleavage facets. Evans and Bache [4] proposed a model to describe facet formation as the result of inhomogeneous strain leading to stress redistribution between "weak" and "strong" orientated grains within the microstructure with respect to the loading direction, fundamentally controlled by the juxtaposition of hexagonal grains of different orientations. In support of the neighbouring grain model, early practitioners of electron back scattered diffraction (EBSD) were able to identify the crystallographic orientations of pertinent grains and it has been widely accepted since that the quasi-cleavage facets form on basal (or at least near basal) planes [5-7].

Ever since the early Farnborough research, all manufacturers of large civil aero-engines have employed the α/β alloy Ti-6Al-4V as the variant of choice for fan disc applications. Notably, different thermo-mechanical processes applied to Ti-6Al-4V can generate a wide variety of α/β microstructures. However, one of the mitigating factors thought to explain an apparently lower level of dwell sensitivity compared to the near alpha alloys was the typical fine grain size relative to near-α variants such as Ti-685, and Ti-829 [8]. The mechanism of quasi-cleavage faceting is encouraged by a large grain size allowing more extensive planar slip [9,10].

Alternatively, the localised concentration of multiple hexagonal grains with a similar basal plane orientation has been recognised to promote dwell fatigue failures in near-α variants such as Ti-834 and Ti-6242 [11,12,13]. Such "macrozones" or "microstructurally textured regions (MTRs)" can be refined through optimised thermo-mechanical processing but this can be more challenging for large section parts [14]. MTRs increase the effective structural unit size in such finer grained alloys. This can be a particular problem when forming large through section engineering components.

The recognition of significant MTRs in full scale Ti-6Al-4V fan disc forgings and their potential role in dwell fatigue failure was highlighted by the failure investigation relating to an in-service disc failure which occurred in 2017, reported in 2020 [15]. Inspection of the fractured disc illustrated a region of contiguous quasi-cleavage facets at the sub-surface crack initiation site. Subsequent metallographic sectioning revealed the presence of significant MTRs immediately below the fracture plane, with the facets associated with underlying, primary α grains with a common basal plane orientation. Sometime before that failure investigation, Venkatesh et al had generated a comprehensive low cycle fatigue (LCF) database from laboratory scale specimens subjected to cyclic and dwell waveforms, eventually published in 2020 [16]. A major objective of their study was to correlate fatigue crack initiation mechanisms to the microstructure and micro-texture found within typical Ti-6Al-4V fan disc forgings [17]. Focussing on two nominal stress conditions, the research deliberately assessed the degree of scatter in measured fatigue lives and the LCF data ultimately confirmed the dwell sensitive nature of Ti-6Al-4V when containing MTRs.

Similar objectives were established during the present study, from which the current data will be presented. Cyclic and dwell LCF experiments were conducted employing a different fan disc forging of similar microstructure and mechanical properties. The current findings are compared to the research reported under [16] to establish the potential for performance variability between different

components. Detailed characterisation is included to demonstrate the critical role of MTRs in the crack initiation process.

Experimental Methods

Plain cylindrical fatigue specimens were extracted from a single fan disc supplied by Rolls-Royce plc. Upset under standard proprietary conditions the pre-machined disc forging had been assigned for destructive microstructural characterisation and mechanical evaluation. A scanning electron microscopy (SEM) image to illustrate the general α/β forged microstructure is included as Figure 1. This was prepared from a random location within the disc bore on the radial-axial plane. Multiple polished sections were prepared at various locations throughout the disc, supporting image analysis measurements of the average primary α grain diameter and % volume fraction primary α at 20μm and 38% respectively.

All rectilinear specimen blanks were extracted with their longitudinal axis in the disc hoop orientation. Two different sized specimen geometries were adopted, Figure 2, on one hand to provide the largest practical cross sectional area / critically stress gauge volume, but also to maximise the number of individual fatigue tests. Throughout this paper these will be designated “large” and “small” specimens, with data from eight of each type reported. In all cases the gauge section was turned using a standard computer encoded control (CNC) machining operation followed by automated longitudinal polishing to provide a surface roughness R_a of 0.4μm or better. Specimen dimensions and concentricity were measured using non contacting optical techniques.

Low cycle fatigue tests were performed under a controlled laboratory temperature of 22°C. Specimens were either subjected to a “cyclic” waveform (15cpm trapezoid, incorporating 1s linear rise and fall ramps with a 1s hold at peak and minimum load) or a “dwell” waveform (the same trapezoidal form but with a 120s hold at peak load). A common load ratio of R=0.05 was employed throughout the test matrix. Data are reported relating to tests performed at two applied peak stress levels. These were set at 870MPa (to directly compare with the highest nominal condition sampled during previous research [16]) and a relatively low stress of 800MPa (with the original expectation to generate dwell failures approximating 20,000 cycles).

All specimens were taken to complete rupture, no run-outs are reported. Post test, optical inspection of the fracture surfaces using the naked eye was often sufficient to confirm the site of crack initiation as surface or sub-surface. However, higher magnification fractography was also performed using a Keyence optical microscope and a Hitachi 3500 scanning electron microscope. Selected specimens were also characterised using EBSD measurements taken directly from the fracture surface to identify the crystallographic orientation of quasi-cleavage facets lying orthogonal to the longitudinal axis of the gauge section. Under this scenario, the SEM equipped with an Oxford Instruments EBSD measurement system was employed, focussed on the fracture surface with the bulk specimen tilted to an angle of 70° relative to the electron beam, set at 20kV and using a 0.9μm step raster.

The same EBSD system was employed to generate more conventional grain orientation maps from polished metallographic sections. These were usually prepared by cross sectioning the gauge of the post tested LCF specimens on an orthogonal plane displaced a few millimetres below the lowest point of the fracture surface. The electron beam step size employed for such maps varied according to the area of interest, desired sampling resolution and the time available to collect data. For relatively extensive maps (e.g. cross sections through the large specimen gauge section) an automated montage mapping facility within Aztec control software was employed. Employing a 20kV electron beam, a step

increment of 0.9μm and optimised system settings returned the best possible zero signal solution (<1.9%). Careful attention was afforded to sample identification, section orientation and precise correlations to adjacent fracture surface features.

Results

LCF Response

The LCF data are plotted on a stress-cycles to failure graph in Figure 3, identified according to cyclic or dwell loading waveforms. The individual data points for specimens tested during the current campaign are compared to the ranges in maximum and minimum life reported for specimens from previous work, based on digitised data from reference [16]. At the relatively high stress level of 870MPa the current dwell tests compare favourably to the mean performance from [16], however, at the same stress the current fatigue strengths measured from cyclic tests correspond to the lower bound of the former data. At the lowest employed stress condition of 800MPa, our strongest dwell specimen fractured at 12,758 cycles, slightly lower than the 20,000 target. Logarithmic trendlines are superimposed on the current cyclic and dwell datasets to emphasise the knock down in strength due to dwell loading. The dwell debit was more significant at the high-stress level of 870 MPa than at the lower stress level. By extrapolation the dwell trendline intersects with the cyclic dataset at approximately 740MPa.

Optical and SEM Fractography

Low magnification optical inspections of the specimen fracture surfaces proved most reliable for identifying the location of fatigue crack initiation and indications of underlying MTRs which may have influenced failure. It should be emphasised that both surface and sub-surface initiations were identified under each mode of loading. A bias was detected, however, with six out eight dwell tests initiating sub-surface and seven out of eight cyclic tests illustrating more traditional LCF initiation sites from the surface. Representative examples of failures imaged at low magnification are presented in Figure 4.

Irrespective of loading waveform and initiation site, the precise location of crack initiation was invariably marked by the presence of multiple quasi-cleavage facets, with the earliest stages of crack growth indicated by diverging river marks within the individual facets. An example is illustrated in Figure 5 using two SEM images obtained at two levels of magnification, adopting the cyclic specimen LC015 from Figure 4. The initiation region is marked by a cluster of juxtaposed facets, each relating to underlying α grains. The facets within the circled region were largely featureless, however, the orientation of local, early crack growth was evident from the river marks within individual facets, as indicated by the superimposed arrows.

Dwell failures were consistently marked by multiple initiation sites. Bright, reflective features were clearly identified under optical inspection, distributed across the eventual macroscopic plane of fracture and alluding to underlying micro-texture, Figure 6. It is informative to recognise that SEM inspection alone often misses the presence of these initiation features, optical low magnification inspection is strongly recommended for the characterisation of dwell fatigue failure modes.

The crystallographic orientation of the individual facets constituting the initiation regions was measured directly off the fracture surface using EBSD measurements. Figure 7 illustrates typical results from cyclic and dwell specimens. In the case of specimen LC015 (cyclic), the general topography of the initiation zone is shown after tilting the specimen to 70° relative to the electron beam.

Alongside, the dominance of basal plane signals emanating from the fracture surface is demonstrated in the associated IPFZ orientation map, with a strong spatial correlation to the orthogonal facetted features. In addition to the strong preference for neighbouring facets to form on a common fracture plane, the corresponding IPFX and IPFY maps also confirmed a strong preference for the underlying α grains to have a common rotation relative to their C axis. For the dwell example, specimen LC017, the initiation region is shown on the left hand side in plan view prior to tilting, whilst the EBSD measurements are overlaid on the tilted view to the right.

A similar exercise applied to an example of surface initiation induced under the cyclic waveform is illustrated in Figure 8. The predominance of basal plane facets orientated orthogonal to the tensile stress axis was once again evident.

Discussion

First, it is worth noting that despite the employment of two different sample geometries, no definitive difference was noted in the fatigue lives measured nor failure mechanisms observed according to the relatively minor difference in the critically stressed volume of these specimens. When designing the test matrix, equal numbers of each geometry were deliberately chosen for cyclic or dwell testing at both stress levels. The location of the test specimen in relation to the disc forging also appeared inconclusive. Therefore, when combined, the findings can be considered to represent a single database, as presented in the current set of graphs and images.

Noting the independent source of materials, the fatigue data generated during the present study compare well to the previous data reported from Venkatesh et al [16], with our dwell data in particular falling close to their previous mean. However, the current cyclic tests tend to congregate near the lower bound (or even slightly below) of the Venkatesh database. The relatively weaker response now reported under cyclic loading could be down to two possible reasons. Firstly, the previous specimens had been shot peened and given crack initiation is biased towards surface initiation under cyclic loading their compressive residual stress presumably resisted initiation and early stage growth. Alternatively, the one second hold at peak stress employed as part of the trapezoidal waveform in this latest study may be pertinent. It could be that this short hold has induced an element of bulk creep and stress relaxation even during the cyclic tests. Recent work on a novel α/β alloy [18] demonstrated a similar frequency effect and the employment of trapezoidal waveforms for the assessment of fundamental LCF performance relative to dwell could be questioned.

Considering the period spent under dwell at the peak of the applied waveform, all of the tests reported here were performed under a two minute dwell. This is a condition that is widely adopted amongst the academic community. A limited number of tests employing a longer dwell period are planned during our on-going project. The initial test we can report was conducted at 800MPa for a dwell period of five minutes. This specimen failed after 6,943 cycles, only marginally shorter than the lower bound of the two minute data at 7,963 cycles. Obviously the database will need to be increased and different stress conditions sampled, but this appears to suggest that prolonging the dwell period beyond a critical time does not induce any more significant damage at this specific stress level. Previous studies have suggested that a significant degree of strain accumulation (under load control) or stress relaxation (under strain control) occurs in this class of material within 30 seconds of holding at peak and beyond that the rate of continued damage/relaxation is very low. Data from Ti-834, also obtained under a peak stress condition of 800MPa but a slightly different R ratio at R=0.1, have previously

shown minimal difference in fatigue life for tests with either two or five minute dwell time. Figure 9 compares the current Ti-6Al-4V data to the Ti-834 data reproduced from reference [19]. The lowest life results for the 1 second (cyclic) and 2 minute dwell conditions are illustrated from the present Ti-6Al-4V data. It is interesting to note that the two alloys demonstrate very similar performance under short dwell time waveforms, however, as the dwell duration is increased to two minutes and beyond it is the Ti-6Al-4V which illustrates marginally superior strength.

Proprietary knowledge of the forging texture, specific to the Trent fan disc supplied for the present research, was considered when fixing the specimen blank positions for manufacture of the two test specimen geometries. Regions of high and low texture (corresponding to different MTR densities) were deliberately sampled. Scrutinising the data plotted in Figure 3, we can confirm that no obvious trends in performance were noted between the large and small specimen geometries. In addition, the general fracture surface appearances were unaffected by the relatively minor differences in the specimen sizes, with multiple MTRs typically exposed across all fracture sections. The large specimens sampled a greater volume of material and the probability of sampling worst case examples of MTRs within the critically stressed gauge section would naturally be increased. However, these larger specimens did not consistently demonstrate the lowest fatigue lives measured at either stress level. Previous laboratory research designed to deliberately consider the role of stressed volume and constraint on dwell response similarly failed to identify clear trends according to specimen size, whilst noting the alloy employed in that study was the coarse grained near α Ti-829 and individual, isolated grains of specific basal plane orientation were responsible for crack initiation in that alloy rather than extensive MTRs [8].

Considering the current data in isolation, the best fit trend lines superimposed on the cyclic and dwell data plotted in Figure 3 indicate that the two data sets merge at an applied peak test stress of approximately 740MPa. Sufficient material was not available to support ancillary strain controlled fatigue testing to define the cyclic yield stress characteristics. However, this laboratory has previously reported data generated from a small diameter Ti-6Al-4V disc with a forged α/β microstructure and the cyclic yield stress of that material was approximately 730MPa [20]. This suggests that the knock down in strength induced under dwell waveforms occurs at stresses above cyclic yield, a phenomenon also reported for the alloy Ti-834 [11]. Therefore, precise knowledge of the cyclic yield stress relating to any alloy in a representative form is vital for the safe design of titanium components if dwell sensitivity is to be avoided. Notably, depending on alloy composition, heat treatment and associated microstructure, the magnitude of the cyclic yield stress could be considerably lower than static (monotonic) yield.

MTRs when exposed on the main fracture surface offer a cross section through three dimensional micro-textured regions contained within the material. Selected specimens were sectioned orthogonal to the gauge as close as possible to the fracture plane and subjected to detailed EBSD mapping. An example relating to the dwell fracture of specimen LC017 is illustrated in Figure 10. Due to the uneven, ductile nature of the failure process the EBSD section was up to 2mm below some areas of the fracture. Clusters of like orientated grains are evident from the EBSD measurements, with their basal 0001 planes lying perpendicular to the applied tensile stress axis (dominated by red in the IPFZ map). Two distinct areas are highlighted (#1 and #2) where the surface facetted zones appear to correspond with underlying MTRs (allowing for slight displacements in radial space). However, an obvious MTR is absent from the inverse pole figure recorded normal to the Z axis orientation (IPFZ) relating to a third zone of surface facets (#3). In a different dwell specimen (LC011) extended, narrow regions of faceting on the fracture surface clearly correspond to linear regions of sub-surface texture, Figure 11. More

detailed examination of the forging flow texture and the relationship to fatigue behaviour is an ongoing area of interest for this project.

Sub-surface initiation should not be taken as *a priori* evidence of a dwell failure. A mix of sub-surface initiation under cyclic loading as well as dwell failures from the surface has been found during the present study on Ti-6Al-4V. Clusters of facets were even responsible for surface initiation under cyclic loading, Figure 8. Similar findings were reported from research employing alternative alloys [18]. The internal microstructure and in particular regions of high crystallographic texture appear to control the random sites of fatigue crack initiation, whether this be surface or sub-surface relative to the gauge section of a laboratory test specimen. In the engineering scenario, the critical region of microstructure will be governed by forging operations, the final machined component geometry and in-service applied stress field. Indeed, when considering examples of fan disc failures, dwell sensitive failures appear to favour sub-surface initiation sites within the thick sections of the bore [15,21]. The increased probability that dwell loading encourages initiation from sub-surface MTRs appears to be related to the increases in bulk creep deformation concentrated within the surrounding randomly oriented microstructure and in the case of components may also be influenced by the bulk residual stress distribution resulting from the forging and heat treatment process. As a time dependent process, the accumulation of damage will naturally occur in fewer cycles under a dwell waveform compared to cyclic loading and authors have demonstrated in a laboratory setting that the magnitude of strain achieved under identical stress conditions is also greater under dwell [22,23].

For the specimens characterised by multiple crack initiation sites it is impossible to define the temporal relationship between the individual cracking events (despite the dominant appearance of some sites compared to others). Indeed, it is probable that additional examples of crack initiation could be present throughout the gauge section, i.e. at sites other than those exposed as the main fracture surface. This has been proven using X-ray computed tomography techniques for this same alloy albeit under scenarios of high cycle fatigue (HCF) [24].

The quasi-cleavage faceting mechanism has received much empirical and modelling attention. It is widely accepted that the facets are the result of load shedding or stress redistribution between weak and strong microstructural features. In the coarse grained alloy variants this can be offered by pairs of juxtaposed grains with differing basal plane orientations. In the weak grain the basal plane is favourably inclined, under a relatively high resolved shear stress, promoting easy planar slip. Dislocations then pile up at the boundary with the neighbouring grain where the basal plane, lying near perpendicular to the tensile axis, is poorly aligned for slip. Eventually, crack initiation occurs in the “strong” grain, orthogonal to the tensile axis. The advent of electron beam milling techniques allowed for the micro-sectioning of neighbouring grains and characterisation of basal slip structures [25,26] confirming the weak-strong intra-grain deformation mechanism. In fine grained variants, with Ti-6Al-4V now definitely included, the mechanical inhomogeneity is provided by extensive regions of contiguous oriented grains forming an MTR alongside regions which can deform relatively easily.

Sophisticated crystallographic characterisation and theoretical arguments have been presented to argue that the slip is actually associated with planes slightly off basal (up to 15°). In response to those arguments we note that;

i) the EBSD technique employed here involved tilting of the bulk specimen to the precise 70° angle relative to the SEM electron beam,
ii) to capture and successfully resolve any Kichuci patterns from the individual facets must prove they lie orthogonal to the tensile stress axis during testing, and

iii) to within the accuracy of the EBSD equipment the vast majority of signals associated with the orthogonal facets were resolved as basal in origin.

Within the extensive clusters of facets associated with the underlying MTRs, the precise location of crack initiation was often identified by tracing the fan like river markings in individual facets back to near featureless or “glassy” facets. The latter are believed to form via planar slip concentrated on a specific crystallographic plane, notably the basal plane, or extremely concentrated slip band within a single grain [27]. In relatively fine grain alloys (e.g. Ti-6Al-4V, Ti-6242 etc) the slip may traverse the entire grain to accentuate the glassy appearance.

On initial inspection by eye, dwell fractures in particular illustrated a highly ductile, dull, fracture surface appearance. Against this background the lustrous regions of facetted MTRs were obvious (see Figures 4 and 6 for examples). The overall fractures were obviously non-planar with significant shear lips formed around the gauge periphery and it was evident that the initiating sub-surface facet clusters were often located on different orthogonal planes (with macroscopic steps formed between). After immediate removal from the mechanical test rig, a few examples appeared “contaminated” to the naked eye, however, this appearance was not affected by standard cleansing in preparation for SEM inspection (i.e. detergent washing in an ultrasonic bath). When subsequently viewed under electron microscopy the opposing halves of the fractured specimen indicated marked peaks and cavities distributed across the opposing fracture surfaces, most notably those specimens tested at 870MPa. Figure 11 shows such features in specimen LC017, indicated by arrows towards the extremities of the dominant macro fatigue crack just prior to tensile overload. However, examples were also found closer to the epicentres of crack initiation. For example, the cavity illustrated at high magnification was located towards the extremity of initiation Zone #1. The facet at the base of the cavity was found to be of basal plane orientation using focussed EBSD spot measurements. The surrounding material has a ductile appearance consistent with the relatively high peak stress applied during this test (870MPa). Although the occurrence of such facetted cavities was also noted at the lower test stress level of 800MPa they were considerably fewer in number.

To avoid any misconception, it is emphasised that these cavities were not an artifact of pre-existing forging porosity. Instead, it is assumed that they originate from local differences in plastic flow behaviour under applied stress. Although the current cavity features are relatively large (tens of microns in diameter) they could be likened to micro-voids formed in ductile metals containing fine precipitation strengthening particles [28]. In contrast to a particle decoherence mechanism but similar to one of particle splitting, the α grain orientated with the basal plane orthogonal to the loading axis appears to be acting as the isolated “strong particle/unit” leading to quasi-cleavage. The grains immediately surrounding it offer multiple and more favourable slip systems thus acting as weaker units. It is also emphasised that these “facetted cavities” were never the epicentre of crack initiation but instead seem to form during the later stages of fatigue crack propagation.

The outcomes from the present study are consistent with the previous laboratory research reported by Venkatesh et al [16] and confirm that Ti-6Al-4V must be considered as a dwell sensitive titanium alloy. In turn, the dwell phenomena described here support the top line conclusion of the investigation relating to the Air France incident reported in 2016 - that dwell sensitive fatigue was the cause of fan disc failure [15]. Notably, evidence that Ti-6Al-4V should not be considered immune to the effects of dwell loading can be found in the long standing literature. Evans demonstrated a dwell debit for two microstructural forms of Ti-6Al-4V back in 1987 [29]. The two microstructural conditions, “annealed α" and “transformed β" both illustrated dwell sensitivity when assessed at relatively high stress levels, above static yield for the respective variants. The same paper refers to LCF testing performed on a

microstructure (most relevant to fan disc components) during the same study. Although fatigue data were not plotted for the α/β variant, it is stated that "….. *the (dwell) sensitivity is evident for all microstructural conditions evaluated …..*" and examples of quasi-cleavage faceting as the cause of crack initiation under creep experimentation as well as fatigue testing of notched geometries were illustrated in the α/β microstructure. Shortly afterwards, Neal also reported a minor effect of dwell fatigue in the α/β variant, although evidence was limited to a single cyclic life condition [30].

It is critical that the aero-engine community consider the potential implications of dwell fatigue for the safe lifing of all in-service Ti-6Al-4V fan discs and future applications.

Conclusions

The following high level conclusions are drawn from the present research:

1. Characterisation of a proprietary Ti-6Al-4V fan disc forging has illustrated the presence of "macrozones" or "microstructurally textured regions (MTRs)".
2. EBSD can be applied to metallographic polished sections or directly from the fracture surface of failed fatigue specimens to identify MTRs.
3. LCF tests have illustrated a debit in fatigue strength if a hold of two minutes is imposed at the peak of the loading waveform.
4. The current data are consistent with a previous database generated on a similar but independently processed Ti-6Al-4V disc forging.
5. The α/β titanium alloy Ti-6Al-4V should be considered as "dwell sensitive" when containing MTRs of the scale investigated during the present study.

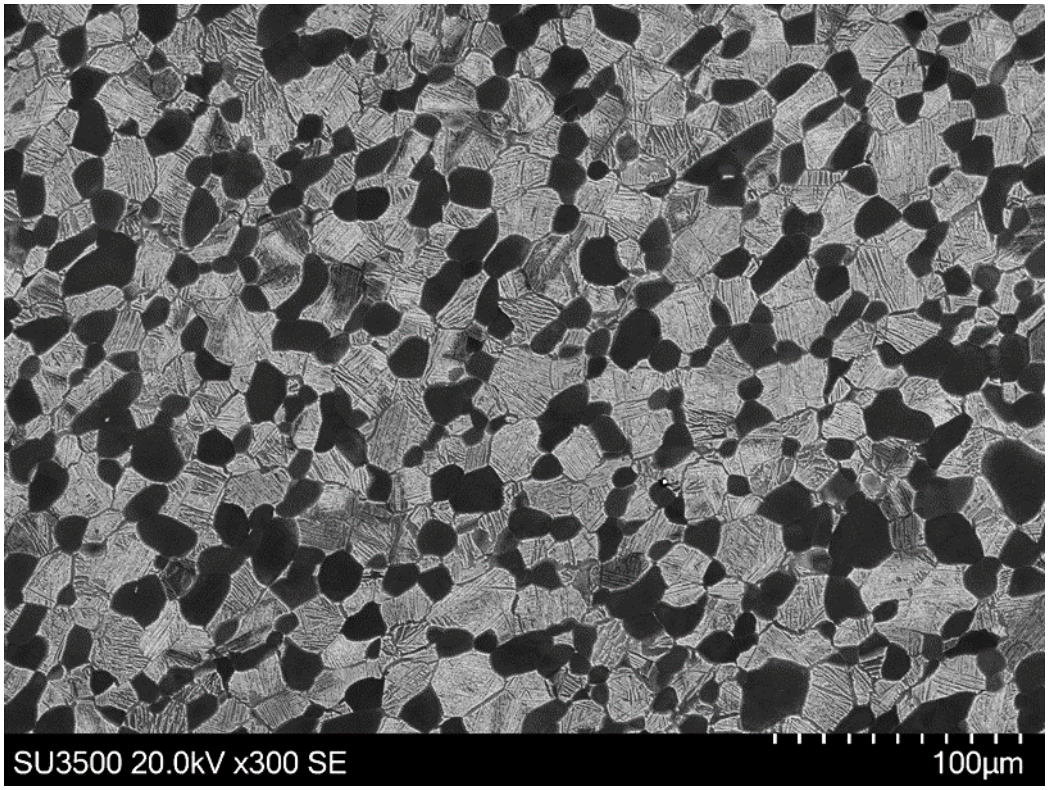

Figure 1. Typical α/β microstructure, sampled within the disc bore. SEM imaging, α phase appears dark, β phase is light.

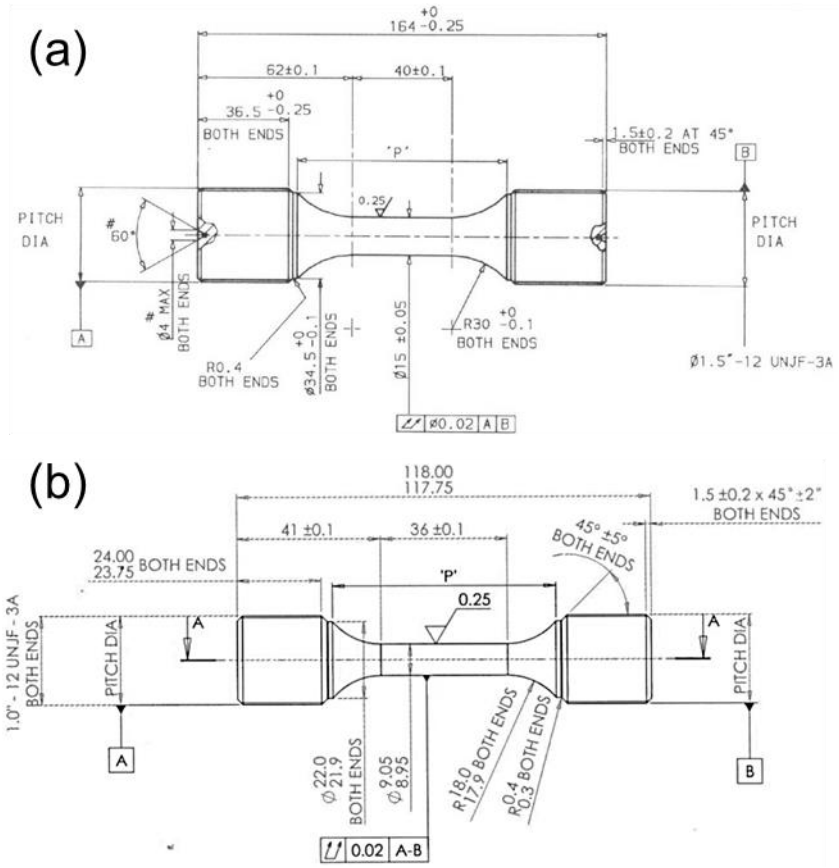

Figure 2. (a) “Large” and (b) “Small” fatigue specimen geometries.

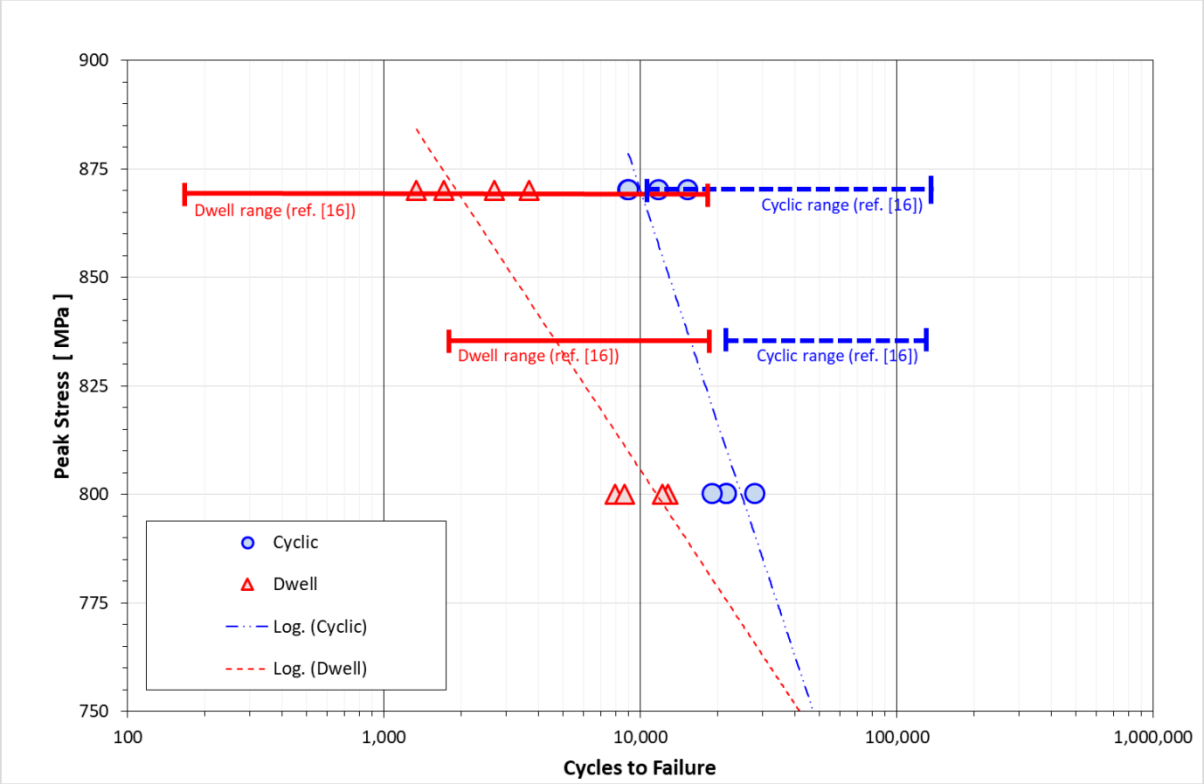

Figure 3. Cyclic and dwell LCF data compared to the ranges in life reported in reference [16].

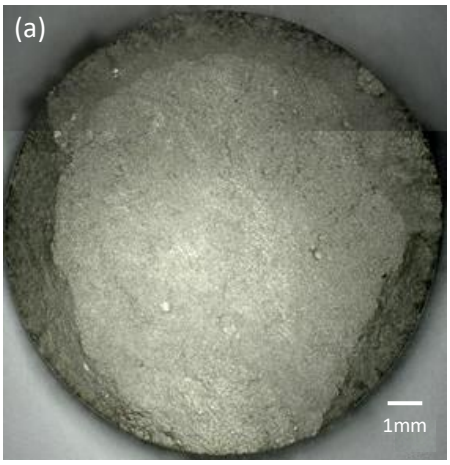

LC016 (cyclic, 870MPa, N_f=8,967)

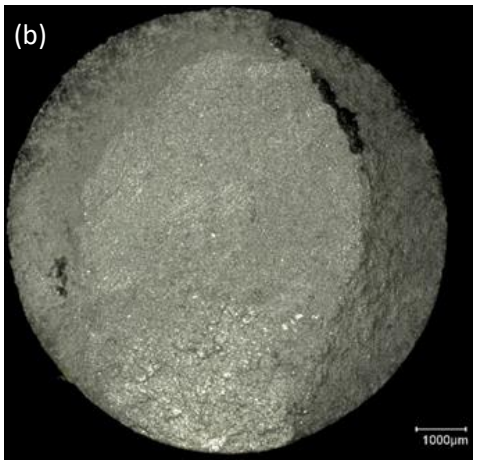

LC001 (dwell, 800MPa, N_f=7,963)

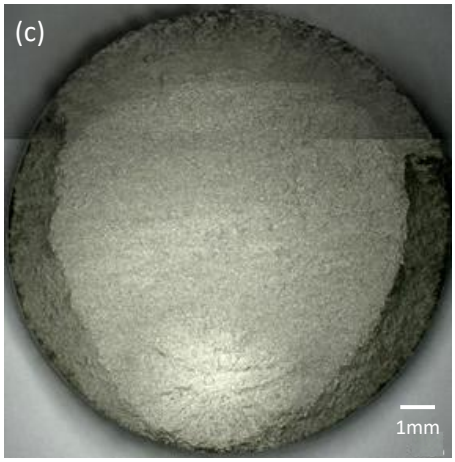

LC015 (cyclic, 870MPa, N_f=15,412)

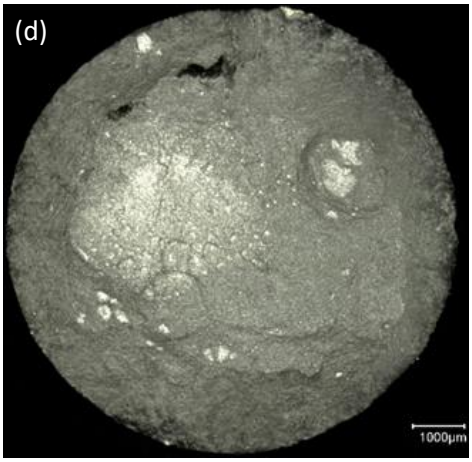

LC006 (dwell, 800MPa, N_f=1,709)

Figure 4. Optical images representing various forms of crack initiation. Surface initiated fractures in a cyclic specimen (a) LC016 (870MPa, N_f=8,967) and dwell specimen (b) LC001 (800MPa, N_f=7,963); Sub-surface initiated fractures in a cyclic specimen (c) LC015 (870MPa, N_f=15,412) and dwell specimen (d) LC006 (800MPa, N_f=1,709).

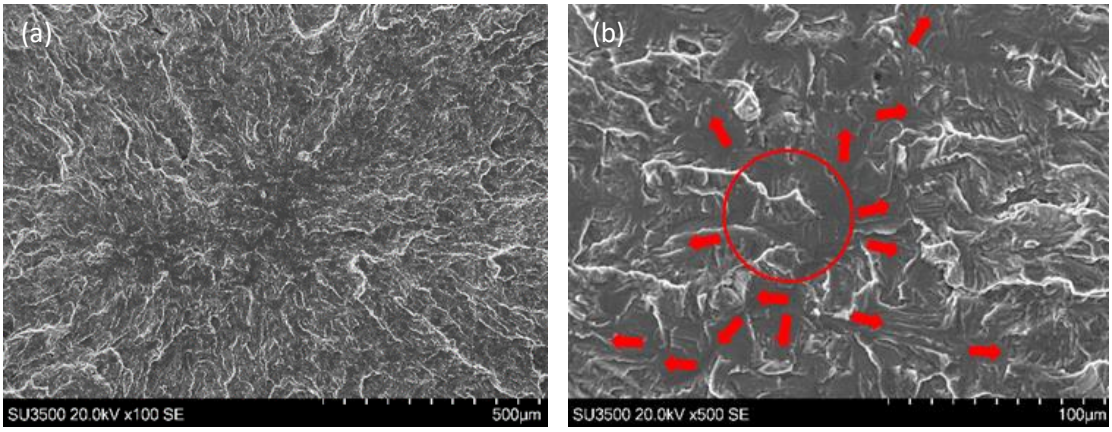

Figure 5. (a) Crack initiation and (b) early growth orientations in specimen LC015 (cyclic waveform, sub-surface initiation site).

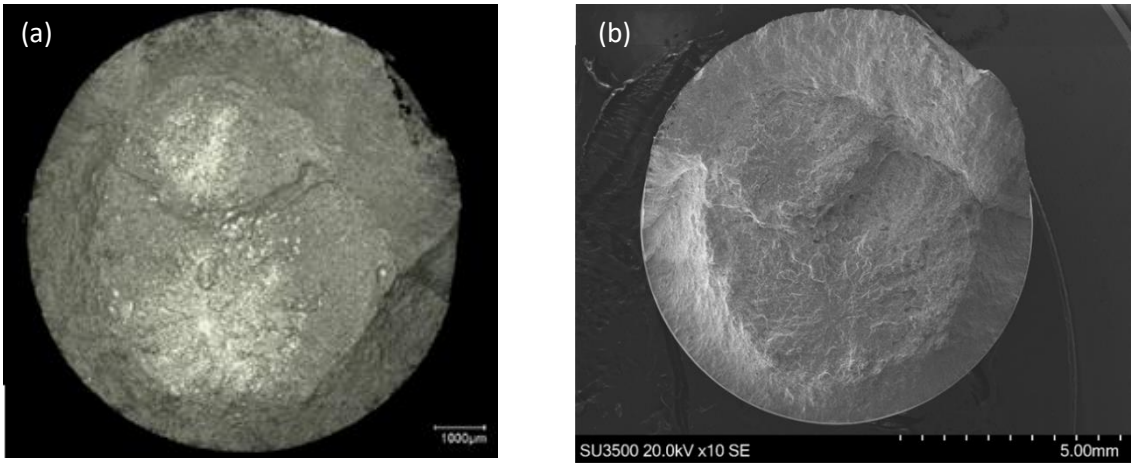

Figure 6. Multiple, sub-surface crack initiation under dwell loading, specimen LC009 (800MPa, N_f=12,201). (a) Optical inspection and (b) SEM inspection.

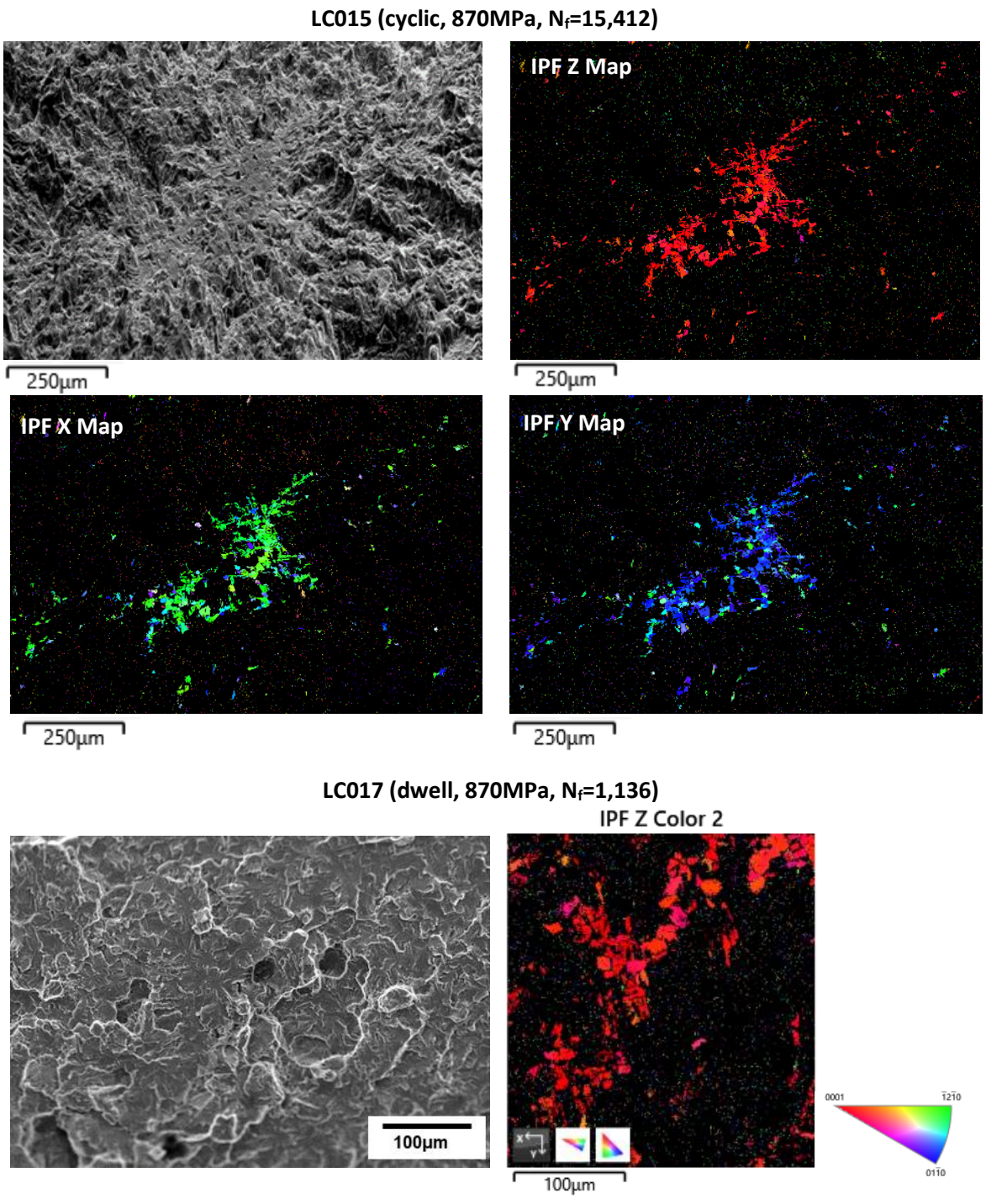

Figure 7. Identification of basal plane facets via EBSD measurements collected directly from sub-surface initiation sites exposed on the fracture surface.

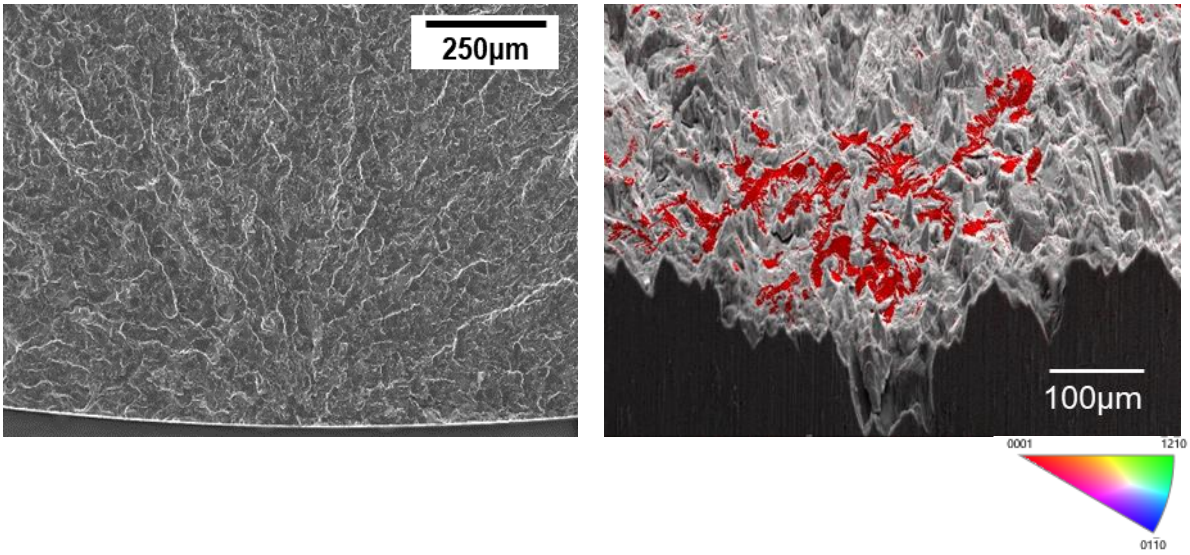

Figure 8. Basal plane facets associated with a surface initiation site formed under the cyclic waveform (LC016).

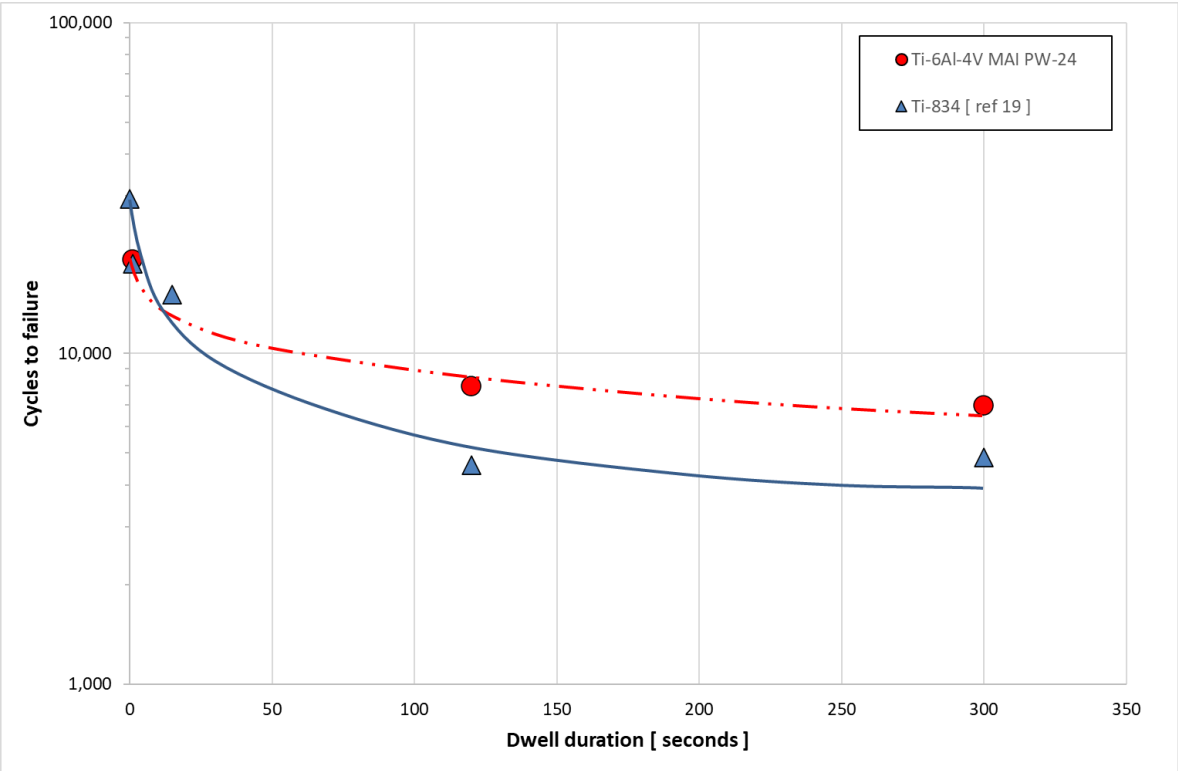

Figure 9. Cycles to failure as a function of dwell duration. All tests were performed at a peak stress of 800MPa. Ti-6Al-4V tests were generated under R=0.05. Ti-834 data were generated at R=0.1 and are reproduced from reference [19]. Trendlines have been superimposed by eye.

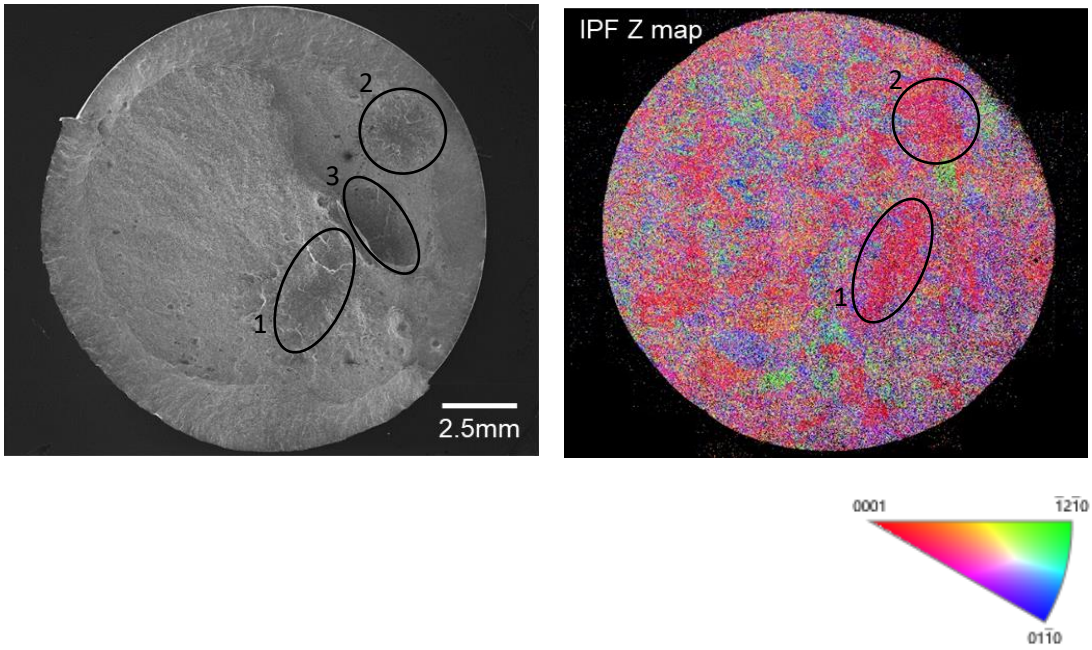

Figure 10. Dwell induced failure in specimen LC017 illustrating obvious MTRs on the fracture surface (left) and associated metallographic section mapped using EBSD (approximately 2mm below the fracture plane).

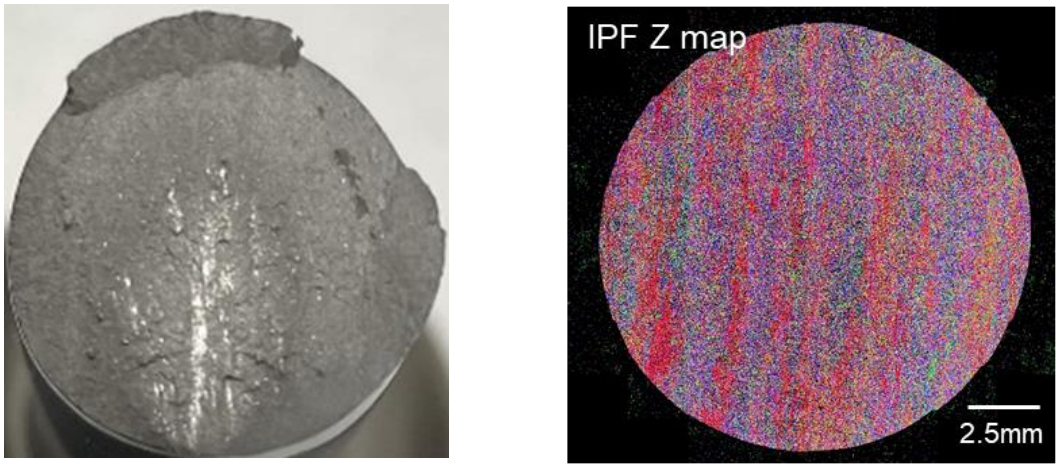

Figure 11. Correlation between elongated zones of fracture surface facets and underlying micro-texture (specimen LC011, dwell, 800MPa).

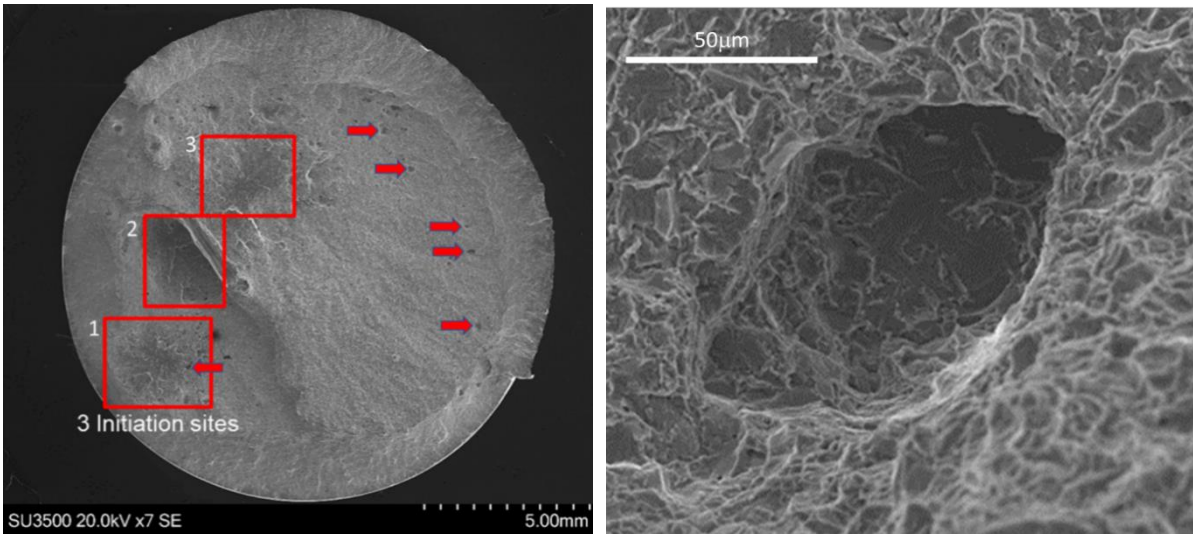

Figure 12. Facetted cavities distributed across the fracture surface of dwell specimen LC017.

Acknowledgements

The current research was funded by the United States Air Force Materials Affordability Initiative (PW-24, contract FA8650-20-2-5224). The provision of Ti-6Al-4V fan disc material by Rolls-Royce plc is gratefully acknowledged. All mechanical testing was performed by Swansea Materials Research & Testing Ltd.

References

1. P. Pugh; “The Magic of a Name, The Rolls-Royce Story, Part 2: The Power Behind the Jets 1945 - 1987”, 2001, Icon Books UK / Totem Books USA
2. W J Evans and C R Gostelow; “The effect of hold time on the fatigue properties of a β-processed titanium alloy”, Metallurgical and Materials Transactions A, Vol 10, (1979), pp. 1837-1846.
3. R. Dutton; “A review of the low-temperature creep behaviour of titanium”, Report AECL-11544 COG-96-70-1, Atomic Energy of Canada Ltd., 1996.
4. W.J. Evans and M.R. Bache, “Dwell-sensitive fatigue under biaxial loads in the near-alpha titanium alloy IMI685”, Int. J. Fatigue, 16, pp.443 - 452, 1994.
5. Somnath Gosh, Mike Mills, Stan Rokhlin, Vikas Sinha, Wolé Soboyejo and Jim Williams; “The Evaluation of Cold Dwell Fatigue in Ti-6242”, final report DOT/FAA/AR-06/24, National Technical Information Service (NTIS), Springfield, Virginia 22161, 2007.
6. M.R. Bache, H.M. Davies and W.J. Evans, “A model for fatigue crack initiation in titanium alloys”, in Titanium ’95: Science and Technology, Eighth World Conference on Titanium, Birmingham, October 1995, Eds. P.A. Blenkinsop, W.J. Evans and H.M. Flower, Institute of Materials (London), pp. 1347–1354, 1996.
7. A.P. Woodfield, M.D. Gorman, J.A. Sutcliff, R.R. Corderman; “Effect of microstructure on dwell fatigue behviour of Ti-6242”, in Fatigue Behaviour of Titanium Alloys, Eds. R.R. Boyer, D. Eylon and G. Lutjering, TMMS, USA, 1998, pp. 111-118.
8. Z.Song and D.W.Hoeppner; “Size effect on the fatigue behaviour of IMI 829 titanium alloy under dwell conditions”, International Journal of Fatigue, Volume 11, Issue 2, March 1989, pp. 85-90.
9. A.N. Stroh; “The formation of cracks as a result of plastic flow”, Proc. Roy. Soc. (London), 223, 1954, pp.404-414.
10. C.C. Wojcik, K.S. Chan and D.A. Koss; “Stage I fatigue crack propagation in a titanium alloy”, Acta Met., 36, pp. 1261-1270, 1988.
11. M.R. Bache, M. Cope, H.M. Davies, W.J. Evans and G. Harrison, “Dwell sensitive fatigue in a near alpha titanium alloy at ambient temperature”, Int. J. Fatigue, 19, Supp. 1, pp. S83-S88, 1997.
12. L. Germain and M.R. Bache, “Crystallographic Texture and the Definition of Effective Structural Unit Size in Titanium Products”, in Ti 2007 Science & Technology, eds. M. Ninomi, S. Akiyama, M. Ikeda, M. Hagiwara and K. Maruyama, The Japan Institute of Metals, 953-956, 2007.
13. A.P. Woodfield, M.D. Gorman, R.R. Corderman, J.A. Sutcliff and B. Yamron; “Effect of microstructure on dwell fatigue behaviour if Ti-6242”, in Titanium ’95: Science and Technology, Eighth World Conference on Titanium, Birmingham, October 1995, Eds. P.A. Blenkinsop, W.J. Evans and H.M. Flower, Institute of Materials (London), pp. 1116-1123, 1996.

14. S.L. Semiatin; “An Overview of the Thermomechanical Processing of α/β Titanium Alloys: Current Status and Future Research Opportunities”, Metall Mater Trans, A 51, pp. 2593–2625, 2020.
15. BEA2017-0568; “Investigation Report: Accident to the AIRBUS A380-861 equipped with Engine Alliance GP7270 engines registered F-HPJE operated by Air France on 30 September 2017 in cruise over Greenland (Denmark)”. Bureau d’Enquêtes et d’Analyses pour la sécurité de l’aviation civile. September 2020
16. V. Venkatesh, R. Noraas, A. Pilchak, S. Tamirisa, K. Calvert, A. Salem, T. Broderick, M.G. Glavicic, I. Dempster and V. Saraf; “Data Driven Tools and Methods for Microtexture Classification and Dwell Fatigue Life Prediction in Dual Phase Titanium Alloys”, MATEC Web of Conferences, 321, 11091 (2020).
17. V. Venkatesh, S. Tamirisa, J. Sartkulvanich, K. Calvert, I. Dempster, V. Saraf, A.A. Salem, S. Rokhlin, T. Broderick, M.G. Glavicic, T. Morton, R. Shankar, A. Pilchak; “ICME of microtexture evolution in dual phase titanium alloys”, Proc. 13th World Conference on Titanium, Eds. Vasisht Venkatesh, Adam L. Pilchak, John E. Allison, Sreeramamurthy Ankem, Rodney Boyer, Julie Christodoulou, Hamish L. Fraser, M. Ashraf Imam, Yoji Kosaka, Henry J. Rack, Amit Chatterjee and Andy Woodfield, TMS (The Minerals, Metals & Materials Society), 2016.
18. W. Davey, M.R. Bache, H.M. Davies, M. Thomas and I. Bermant-Parr; “Fatigue Performance of the Novel Titanium Alloy TIMETAL®407”, in Proc. 14th World Titanium Conference, June 2019, Matec Web of Conferences, Nantes, France.
19. W.J. Evans; “Optimising mechanical properties in alpha + beta titanium alloys”, Mat. Sci. Engineering, A243, pp. 89-96, 1998.
20. M.R. Bache and M. Tasleem; “Fatigue life prediction techniques for notch geometries in titanium alloys”, International Journal of Fatigue, 21 (1999), pp. S187–S197.
21. Harrison, G.F., Tranter, P.H., and Evans, W.J.; “Designing for dwell sensitive fatigue in near alpha titanium alloys”, Proc. Int. Metal. Conf. Designing with Titanium, Bristol, 1986.
22. C. Lavogiez , S. Hémery and P. Villechaise; “On the mechanism of fatigue and dwell-fatigue crack initiation in Ti-6Al-4V”, Scripta Materialia, Vol. 183, 2020, pp. 117-121.
23. M.R. Bache and W.J. Evans; “Dwell sensitive fatigue response of titanium alloys for power plant applications”, Transactions of ASME 2001-GT-0424, J. Eng. For Gas Turbines and Power, 125, pp. 241-245, 2003.
24. Fumiyoshi Yoshinaka, Takashi Nakamura, Shinya Nakayama, Daiki Shiozawa, Yoshikazu Nakai and Kentaro Uesugi; “Non-destructive observation of internal fatigue crack growth in Ti–6Al–4V by using synchrotron radiation μCT imaging”, International Journal of Fatigue, Volume 93, Part 2, December 2016, pp. 397-405.
25. M.R. Bache, C. Pleydell-Pearce, R. Ding & I.P. Jones; “Crystal Plasticity and Quasi-Cleavage Facet Formation During Fatigue Loading proceedings of the 12th World Conference on Titanium, Eds. L. Zhou, Hui Chang, Yafeng Lu, Dongsheng Xu (Ti-2011), June 19-24, Bejing, China, pp. 1152-55.
26. Xu, Y., Joseph, S., Karamched, P. et al. Predicting dwell fatigue life in titanium alloys using modelling and experiment. Nat Commun 11, 5868 (2020).
27. A.L. Pilchak, M.C. Brandes, R.E.A. Williams and J.C. Williams; “Investigation of facetted crack initiation and propagation in near-alpha titanium alloys”, in Ti 2011 - Proceedings of the 12th World Conference on Titanium, Eds. L. Zhou, Hui Chang, Yafeng Lu, Dongsheng Xu, June 19-24, Bejing, China, pp. 993-997.
28. W.D. Callister Jr.; “*Materials Science and Engineering : An Introduction*” (5th ed.), 2000.

29. W.J. Evans; “Creep-fatigue interactions in Ti-6Al-4V at ambient temperatures”, in Proc. 3rd International Conference on Creep and Fracture in Engineering Materials and Structures, Eds. B. Wilshire and R.W. Evans, Institute of Materials (London), pp. 603-613, 1987.
30. D. Neal; “Creep fatigue interactions in titanium alloys”, in Proc. 6th World Conference on Titanium, Cannes, June 6-9, 1988, Eds. P. Lacombe, R. Tricot and G.Béranger, Société Française de Métallurgie, Les Editions de Physique, France, 1989, pp. 175-180.